Hindawi
Shock and Vibration
Volume 2017, Article ID 8932149, 13 pages
https://doi.org/10.1155/2017/8932149

Research Article

The Monitoring of Palazzo Lombardia in Milan

Marta Berardengo,[1] Giorgio Busca,[2] Simone Grossi,[2] Stefano Manzoni,[2] and Marcello Vanali[1]

[1]*Dipartimento di Ingegneria e Architettura, Università di Parma, Parma, Italy*
[2]*Dipartimento di Meccanica, Politecnico di Milano, Milano, Italy*

Correspondence should be addressed to Marcello Vanali; marcello.vanali@unipr.it

Received 27 June 2017; Revised 19 September 2017; Accepted 28 September 2017; Published 24 October 2017

Academic Editor: Michele Palermo

This paper discusses the monitoring of Palazzo Lombardia, one of the tallest high-rise buildings in Italy. First, the layout of the monitoring system is addressed for a general description of the sensors used. The paper provides details about how data coming from transducers are used. Special focus is put on the use of signals acquired by means of accelerometers, which are employed for the estimation of modal parameters through operational modal analysis. The procedure used for choosing the modal analysis algorithm and fixing the values of its main parameters is discussed in detail. The modal identification results on the first eight months of monitoring are discussed in the second part of the manuscript, together with a statistical analysis. This allows for a first model of the relationships between eigenfrequencies and environmental variables aiming at a general structural health monitoring procedure based on the evolution of the building's modal parameters.

1. Introduction

Structural health monitoring (SHM) is the discipline aiming at finding reliable strategies to assess the healthy condition of civil and mechanical structures [1]. For the last two decades, this research field has attracted the attention of many researchers because of the significant outcomes in case of success of this new approach to maintenance. The main advantage of using these techniques is the possibility to switch from a time-based maintenance to a condition-based method [2]. If maintenance was based on measurements collected from the structure, it would be possible to repair structural elements only when really needed. The main advantage is economic, but the consequence on safety of structures is also significant. These techniques allow establishing continuous monitoring systems on important structures such as flyovers, damps, and power stations to enhance their reliability during normal operational life and after extraordinary events such as earthquakes.

Damage identification could be performed at five different levels of detail: simply detecting the presence of damage and its localization, evaluating the type of damage, quantifying its entity, and finally estimating the residual life [3]. The general process to achieve these aims is based on the acquisition of data from several sensors fixed to the structure and the elaboration of this information in order to estimate one or more features sensitive to damage. Since damage could be seen as a stiffness reduction or the inception of nonlinear behaviour, for instance, due to a crack, a common strategy is to measure vibrations and extract damage features from the dynamic response of the structure in operational conditions [4]. Depending on the method used to evaluate the presence of damage, strategies for SHM can be roughly divided into two groups: model-based and data-driven [3]. The former detects damage by evaluating the difference between features extracted from the real structure and those coming from a physical model that should be as much accurate as possible. The latter usually identifies damage through a statistical comparison between features coming from an unknown scenario of the monitored structure and those coming from its healthy condition.

For civil structures, both approaches can be used, though methods based on physical models are usually more popular because they can achieve all the five levels of damage identification and because of the strong experience of civil engineers in building reliable models. Among model-based strategies,

linear methods are well-established techniques that are based on simple assumptions: damage is a stiffness reduction which modifies the structural dynamic parameters such as vibration frequencies [5–7], mode shapes and their curvatures [8–11], flexibility matrix [12–14], and modal strain energy [15–17]. However, the accuracy of these methods in finding damage, especially at their first stage of inception, depends on the uncertainty of modal parameter identification and the variation of structural properties due to the environmental conditions [18–22].

Normally, in the context of SHM, dynamic parameters such as natural frequencies and mode shapes are identified from the dynamic response of the structure in operational conditions [23, 24]. This requirement comes from the necessity to keep the structure accessible to the public but having a continuous control of its health condition at the same time. Operational modal analysis (OMA) is an only-output technique that can estimate modal parameters without using any actuator [25–27]. This property is advantageous because usually actuators are bulky machineries that require closing the structure to the public. However, the quality of the identification strongly depends on the noise affecting the signals and the frequency resolution of the data used for the analysis. Generally, incipient damage produces a slight change of modal parameters; then it is fundamental to keep the estimation uncertainty under control to detect a small anomaly in modal parameters.

Beyond the uncertainty of modal identification process, another issue that can nullify damage detection is the effect of environmental conditions. Modal parameters, especially eigenfrequencies, might strongly change because of a variation of the environmental conditions such as temperature, humidity, and wind speed. If these variables cannot be filtered out from the damage identification process, two scenarios could happen: the variation of the modal parameters generated by the environment could be recognised as damage without any reason or the variation due to the environmental conditions could cover damage which is actually present in the structure.

In this context, this paper offers a study based on the data collected from the new skyscraper of the Lombardia Regional Government. This building is made up of 42 floors and it is equipped with a continuous monitoring system collecting data from several accelerometers and inclinometers. Since the monitored floors are just 5 (see Section 2), it is not convenient to use mode shapes for SHM purposes. Indeed, the aim of this work is to explore the use of frequencies as damage features focusing on the qualification of the modal identification uncertainty and the effects of the environmental conditions. However, also mode shapes are taken into account because the number of sensors could be increased in the near future with the consequent possible use of mode shapes for SHM purposes as well.

The paper is structured as follows. Section 2 describes the structure and the layout of the monitoring system. Section 3 discusses the identification algorithms considered and the characterisation of their accuracy. Section 4 presents the results of the modal parameter identification carried out on the first eight months of the operation of the monitoring system. Finally, Section 5 presents a first-attempt empirical model to link the eigenfrequency behaviour to environmental factors.

2. Layout of the Monitoring System

The Palazzo Lombardia building is the first in a series of high-rise buildings that have been built in Milano in the last years. It is the current seat for the Regional Government and therefore is considered of strategic relevance. The complex is made up of five lower buildings (about 40 m high, called Cores 2, 3, 4, 5, and 6), surrounding the high-rise tower (Core 1), which scored, at the time of construction, the new height record in Italy (161 m). The monitoring system is targeted to control Core 1 tower and is capable of handling both dynamic vibration signals and static variables, as well as the wind conditions. Figure 1 shows a schematic representation of the system layout, while a full description of the installed sensor network and its performances can be found in [28].

Five floors are instrumented with inclinometers and accelerometers according to the general layout given in Figure 1. The setup was designed in accordance with the dynamic testing results [29] in order to be able to identify at least the first three vibration modes and to asses wind comfort issues.

In order to be able to monitor vibration comfort levels against wind serviceability and perform continuous operational modal analysis identifications, very high sensitivity low noise accelerometers had to be employed. Moreover, the building's first natural frequency is around 0.3 Hz, thus posing problems on both the sensor choice and the data acquisition hardware. Since a cabled solution has been chosen (synchronized wireless measurements were not considered affordable on such a high building), the sensor types were chosen in order to minimize the needed cabling.

On the other hand, the selected tilt sensors had to provide long-term stability and a certified temperature sensitivity in order to guarantee reliability to the static measurements.

According to all the above stated needs, the following sensors were chosen:

(i) Accelerometers: PCB 393B31 piezoelectric units, which have been proven to have a very low noise floor level and guarantee good frequency response down to 0.1 Hz, having a 4.9 m/s^2 full scale value

(ii) Inclinometers: ±5° Singer TS servo-inclinometers with extended temperature calibration. They are high reliability sensors with a frequency response up to 3 Hz, which is enough to cover the building's first frequencies

(iii) Wind speed/direction: anemometer NESA ANS-VV1-A + ANS-DVE-A (potentiometric wind direction), with a 50 m/s full scale value

Data acquisition is performed 24 h per day with a final sampling frequency of 250 Hz on all the channels. This is enough to asses wind comfort and vibration disturbances and provide data to modal analysis purposes [25, 30–32]. The data acquisition device is Field-Programmable Gate

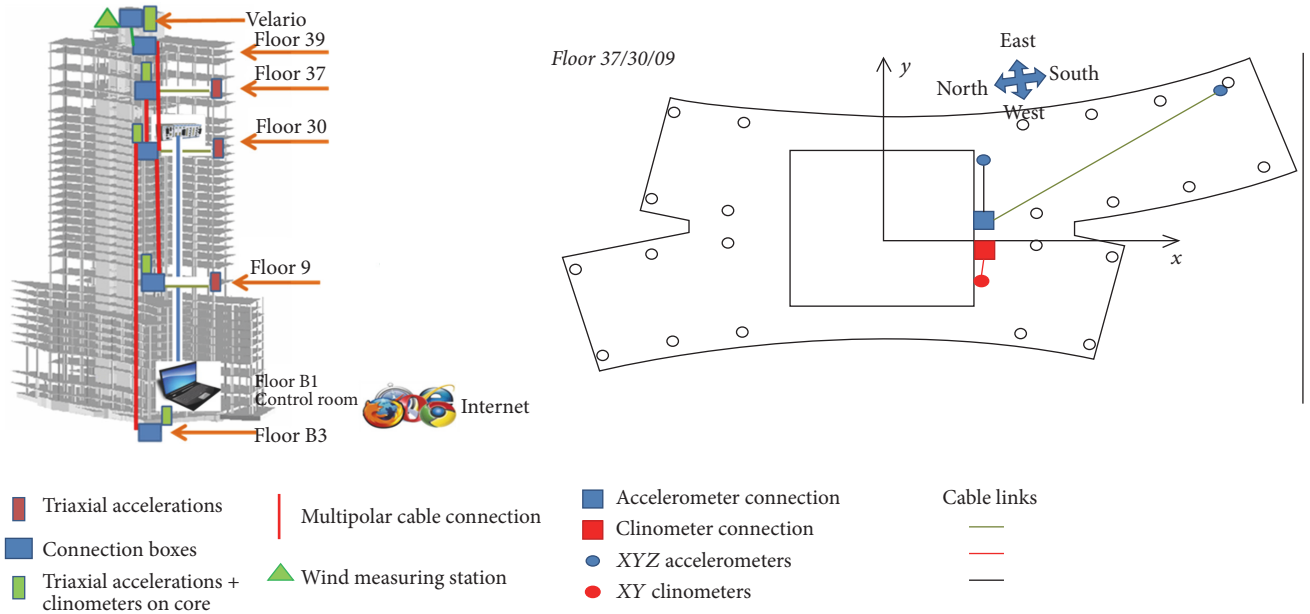

FIGURE 1: Layout of the monitoring system. Floor B3 and Velario differ from floors 37/30/09 because of the lack of the external accelerometers. In each accelerometer location, there are three accelerometers measuring in x, y, and z (out of the figure) directions. In inclinometer location, there are two inclinometers measuring around the x and y axes.

Array (FPGA) based, using 24-bit converters and built-in antialiasing filters.

A total of 24 high sensitivity piezoelectric accelerometers and 10 inclinometers are installed along the whole building together with the wind measurement station on top of it. A new data file is generated every 10 minutes ready to be analysed. This monitoring system is also integrated with some temperature and radiation power sensors previously installed in the building.

3. Identification of Modal Parameters

As described in the previous section, the monitoring system is made from inclinometers, accelerometers, and transducers for environmental variables (e.g., temperature, wind strength, and direction). One of the approaches used for monitoring the building is the continuous modal parameter identification using the accelerometer signals, coupled to the analysis of the data collected by means of the inclinometers. The modal data are employed to investigate the dynamic behaviour of the structure, while the signals provided by the inclinometers are used to describe its static behaviour.

The modal extraction is performed by means of OMA. This is a very attractive approach when monitoring huge structures because it allows considering the unmeasured environmental excitation as the source to force the system (e.g., [33–40]). This section focuses on the choice of the algorithm used to carry out modal extraction. Two different algorithms were tested: the polyreference least-squares complex-frequency (pLSCF) domain method and a method based on the frequency domain decomposition (FDD), which relies on the singular value decomposition (SVD). The two methods are compared in terms of dispersion and bias effects on the estimated modal parameters using the Markov Chain Monte Carlo (MCMC) method. This analysis also allowed finding the optimal values for the parameters used in the analysis of the real data.

3.1. OMA Algorithms. The two algorithms that were taken into account are the pLSCF and the FDD, as already mentioned. They are briefly discussed here to provide the most relevant information. More details can be found in the referenced works.

With regard to pLSCF, one of its main properties is that it provides clean and easy-to-interpret stabilization diagrams and this reduces the amount of complexity for its use as well as difficulties for getting reliable results. This has caused the pLSCF to become the industrial standard for modal analysis at the present time [25, 26]. pLSCF is a least-squares approach in frequency and can be used in OMA. In this case, the inputs to the method are the positive power spectra of the system responses [25].

The second algorithm taken into consideration is the FDD. As mentioned, it is based on SVD. SVD [41] is a linear algebra technique that can achieve factorization of a complex matrix. FDD identification method works by decomposing the power spectral density (PSD) matrix in its principal components at each spectral line. More details can be found in the wide referenced literature (e.g., [25, 27]).

There are two parameters which must be considered as inputs when using the two mentioned OMA identification approaches: the frequency resolution R of the power spectra and the number of averages N used to calculate them [42]. It is known in the literature that a narrow frequency resolution allows improving the accuracy of the modal identification. It is also easy to understand that the higher the number of

Table 1: Reference parameters for the Monte Carlo simulations.

First eigenfrequency	First mode shape	Second eigenfrequency	Second mode shape	Third eigenfrequency	Third mode shape
0.32 Hz	Bending (east-west direction)	0.40 Hz	Bending (north-south direction)	0.63 Hz	Torsion

averages is, the cleaner the power spectra will be and the more reliable the modal identification will thus be. This would suggest increasing the time length of the acceleration signals used to calculate the power spectra. Indeed, if T_t is the total time of the acceleration time histories used for the modal extraction and if the whole time records are divided into N subrecords of time length t_t (with no overlap), it results that

$$R = \frac{1}{t_t} = \frac{N}{T_t} \Longrightarrow T_t = \frac{N}{R}. \quad (1)$$

Therefore, T_t must be increased in order to both increase N and decrease R.

However, T_t cannot be increased indefinitely because the structure changes its behaviour in time: for example, the modal parameters of a structure change between day and night due to thermal shifts. Hence, a high value of T_t would lead to results of OMA which would be a sort of averaged result, preventing the description of the time trends of the identified modal parameters. Therefore, it is important to choose T_t not too high for describing the modal behaviour of the structure in time; at the same time, T_t must be not too low because this would cause a poor accuracy on the identified modal parameters. According to these points, a maximum possible value for T_t was fixed equal to 10800 s (i.e., 3 hours), which is a time span over which an initial data check did not evidence any significant effect of the environmental conditions. Once this threshold was fixed, the effects of different values of R and N were studied by means of MCMC simulations. These simulations and their results are described in Section 3.2.

3.2. Markov Chain Monte Carlo Simulations. The comparison of pLSCF and FDD was carried out by means of the MCMC method. Time histories of accelerations were generated numerically with the goal to make them as close as possible to those collected by the accelerometers placed in the building. Then these numerical time records were provided as inputs to the two algorithms.

These simulated signals were generated by means of a modal model of the structure, considering the first three modes. The data used to build such a model came from a former modal analysis carried out just after the building construction (see Table 1) [29]. The PSDs of the generated signals were made as close as possible to the PDSs of the actual signals collected by the accelerometers. The reference actual PSDs were chosen from a day with very low wind in order to test the case with the poorest signal-to-noise ratio.

The effect of the electrical noise due to the transducers, cables, and so forth was taken into account as well. Indeed, random noise was added to the generated signals and this allowed testing the modal extraction in situations close to the real application. The PSD of the added random noise was obtained from the accelerometer and acquisition board data sheets.

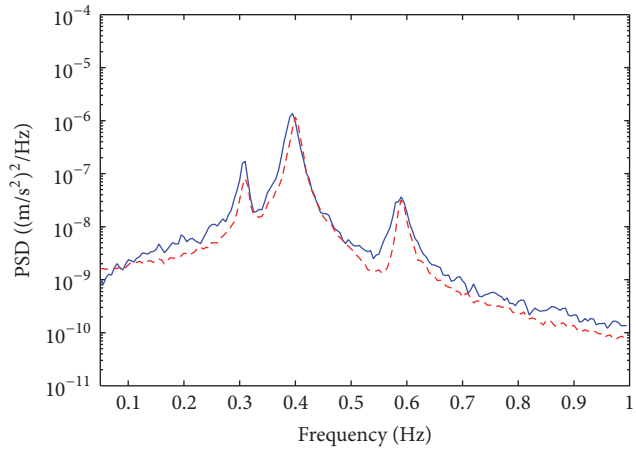

Figure 2: Experimental (solid curve) and numerical (dashed curve) PSD for an accelerometer on floor 30 in case of low wind.

Figure 2 shows a comparison between a PSD of a simulated signal and a real one. The agreement is satisfactory. Obviously, since the signals are of random nature, Hanning window was always used [43, 44] to process the time signals before passing in the frequency domain. This figure also shows that the value of the numerical PSD curve far from the resonances is close to the experimental one. This proves that the amount of random noise added to the numerical signals was correct.

The signal generation for each configuration tested (i.e., fixed values of N and R) was repeated 300 times. Then, modal identification was carried out for each iteration. The focus of the analysis was on the estimation of eigenfrequencies and mode shape components. Since the mode shape vectors are made from many numbers (i.e., many eigenvector components), the results related to mode shapes were described by a synthetic index: the modal assurance criterion (MAC) [41] between the identified mode shapes and the reference ones used in the modal model.

This procedure allowed us to build statistical populations for the following indexes:

(i) Errors between estimated and reference eigenfrequency values: these errors account for bias on the estimations by computing the population mean values μ and for the dispersion of the estimation by employing the standard deviation σ

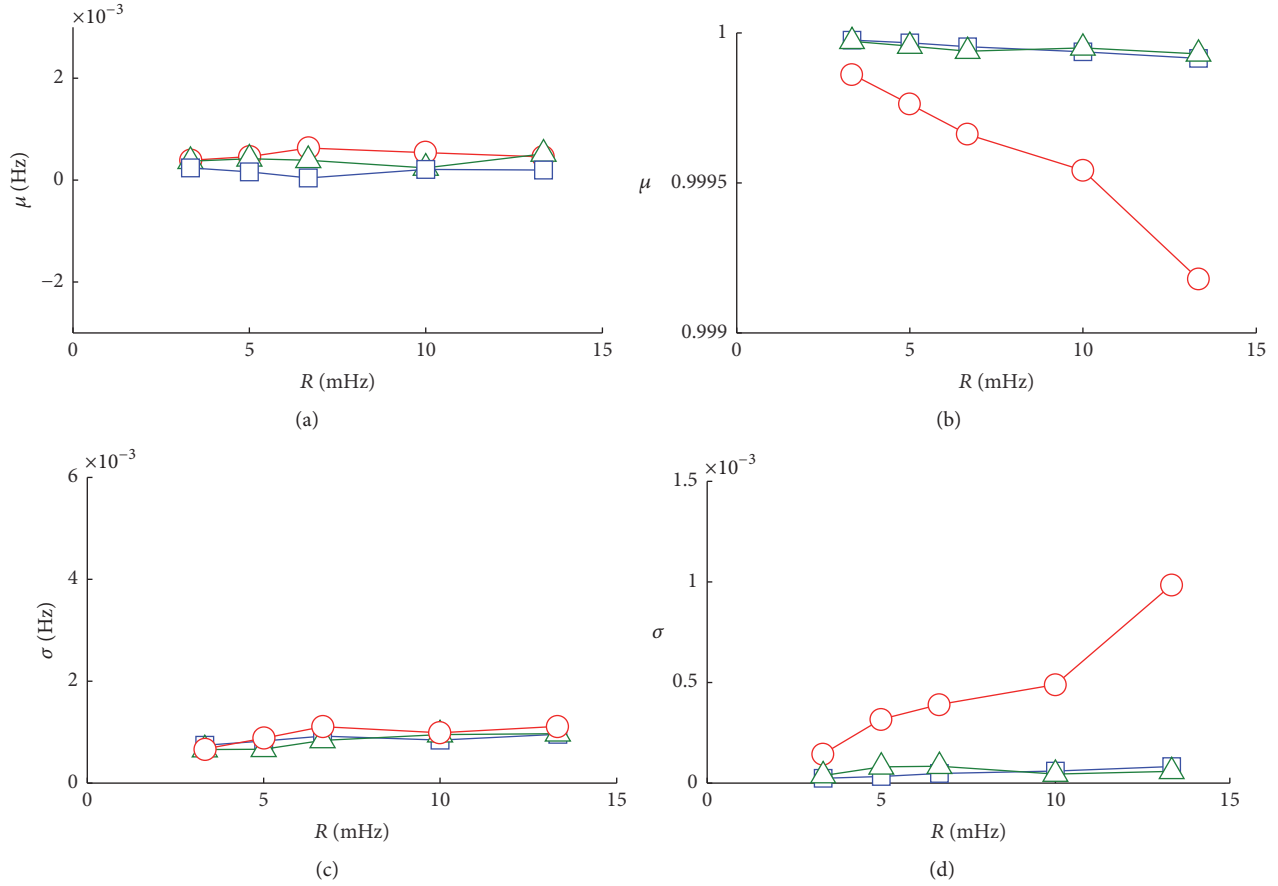

Figure 3: Results of the MCMC simulations for pLSCF as function of R ($N = 36$): mean value of the error for the eigenfrequency estimation (a), mean value of the MAC (b), σ of the error for the eigenfrequency estimation (c), and σ for the MAC (d). Curves with squares (□) for the first mode, with circles (○) for the second mode, and with triangles (△) for the third mode.

(ii) MAC value: the mean MAC value μ accounts for bias, while again dispersion is related to the standard deviation σ of the MAC populations

The trends of these mean and standard deviation values were investigated as function of two input variables: the number of averages N and the frequency resolution R employed to calculate the power spectra provided as inputs to the modal identification algorithms. The populations of the errors on the eigenfrequencies and each eigenvector component were almost Gaussian. It is important to remark that the MAC results obviously show nonsymmetric populations. This means that the value of σ associated with the MAC populations cannot be directly related to any confidence interval of the estimates (an identification of the type of distribution would be required). However, the value of σ for the MAC is shown here for the sake of conciseness to provide an indication about the dispersion of the results in place of showing the standard deviation related to each eigenmode component (which would be correct under a metrological point of view).

Table 2 shows the limit values of R and N tested in the MCMC simulations. Each of the selected R-N pairs was such that the limit on the total time history, 10800 s, was satisfied; therefore, the pairs leading to T_t higher than 10800 s were discarded (an exception was made for few pairs considered for checking the results). It is noticed that in this case overlap between two subsequent subrecords was not used to increase N for a given value of R. The value of the overlap V was thus always equal to 0% [43].

Table 2: Values of T_t, R, and N tested in the Monte Carlo simulations.

Tested values of T_t [s]	Tested values of N	Tested values of R [mHz]
From 1000 to 10800	From 13 to 72	From 3.3 to 13

Figures 3–6 show the results in terms of μ and σ for the first three modes of the building as function of the frequency resolution and the number of averages. Particularly, Figures 3 and 4 show the results for pLSCF, while Figures 5 and 6 show the results for FDD.

The analysis of these figures suggests the use of pLSCF for estimating the eigenfrequencies. Conversely, the FDD is more accurate for identifying mode shapes. With regard to eigenfrequencies, the values of μ of the differences between

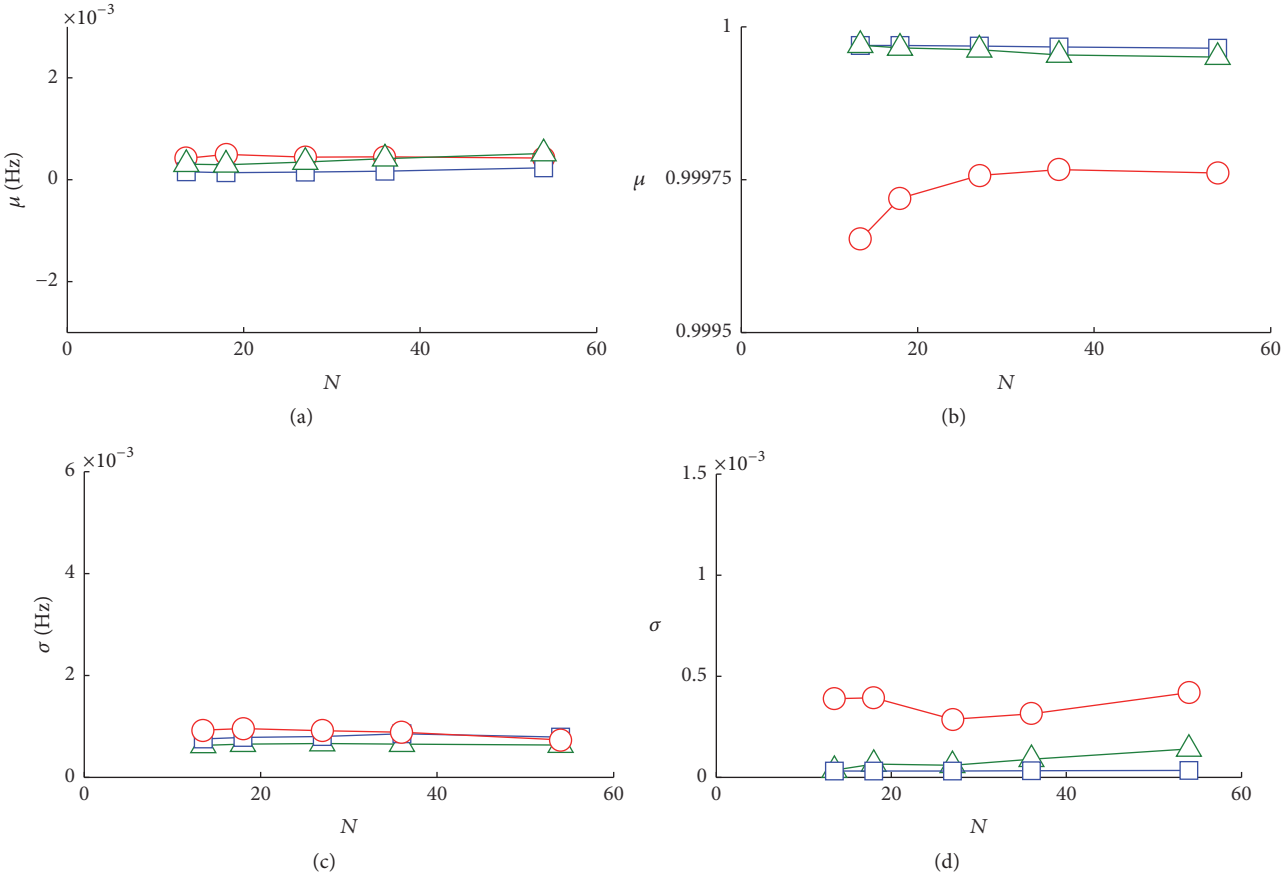

FIGURE 4: Results of the MCMC simulations for pLSCF as function of N ($R = 5$ mHz): mean value of the error for the eigenfrequency estimation (a), mean value of the MAC (b), σ of the error for the eigenfrequency estimation (c), and σ for the MAC (d). Curves with squares (□) for the first mode, with circles (○) for the second mode, and with triangles (△) for the third mode.

estimated and reference values are similar for the two algorithms (and negligible). Conversely, the dispersion of the error is much lower in the case of the pLSCF (see Figures 3(a), 3(c), 4(a), 4(c), 5(a), 5(c), 6(a), and 6(c)). As for the MAC, the FDD provides better results for the second mode (see Figures 3(b), 3(d), 4(b), 4(d), 5(b), 5(d), 6(b), and 6(d)). Therefore, a mixed approach was used when analysing real data: the use of pLSCF for identifying poles (and thus eigenfrequencies) and then FDD for the mode shape components.

Therefore, choosing a mixed approach allows improving the accuracy associated with the estimated modal quantities. The MCMC simulation also allowed finding reliable data about the effect of frequency resolution and number of averages of the power spectra and thus choosing properly their values (see Table 3). The bias values associated with the identified eigenfrequencies are very low, as evidenced by Figures 3(a) and 4(a). Instead, the expected values of the dispersion associated with the identified eigenfrequencies are gathered in Table 4 and can be used as an estimation of the uncertainty of the identification method [45].

It is remarked that, for the configuration of values of Table 3, the MCMC test was repeated with a higher number of simulations (using an adaptive version of the MCMC [46]) to assess statistical reliability. The results obtained are almost the same as those already shown with 300 simulations.

TABLE 3: Chosen values of T_t, R, and N to be used in OMA with real signals.

Chosen value of T_t [s]	Chosen value of N	Chosen value of R [mHz]
7200	36	5

TABLE 4: Expected values of σ on the eigenfrequency estimations.

σ on the first eigenfrequency	σ on the second eigenfrequency	σ on the third eigenfrequency
0.8 mHz	0.8 mHz	0.6 mHz

4. Trend of the Identified Modal Parameters for the High-Rise Building

The values of R and N chosen with the MCMC simulations, as well as the use of the mixed approach pLSCF/FDD, allowed developing an automatic OMA identification system. To do

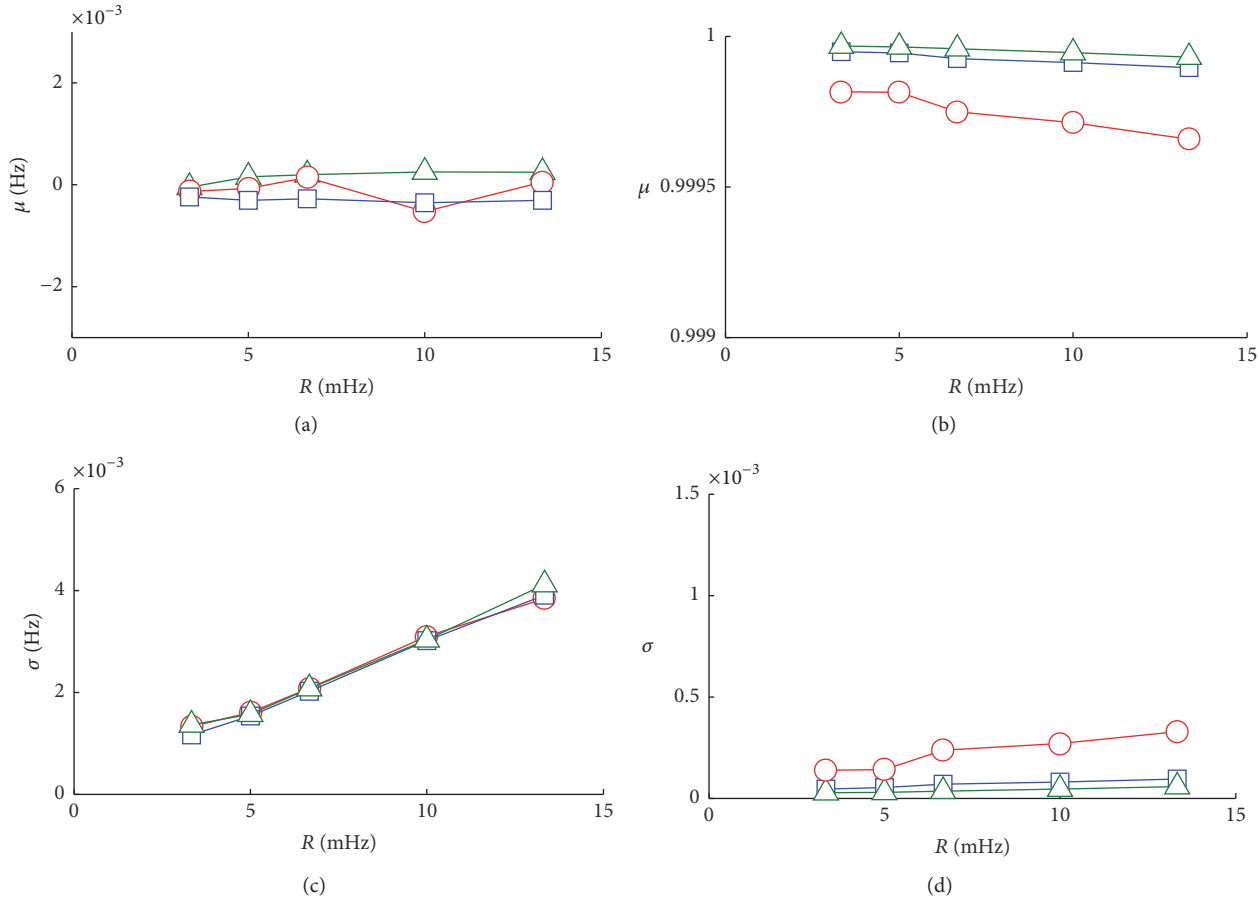

FIGURE 5: Results of the MCMC simulations for FDD as function of R: mean value of the error for the eigenfrequency estimation ($N = 48$) (a), mean value of the MAC ($N = 36$) (b), σ of the error for the eigenfrequency estimation ($N = 48$) (c), and σ for the MAC ($N = 36$) (d). Curves with squares (□) for the first mode, with circles (○) for the second mode, and with triangles (△) for the third mode.

this, an automated data check procedure was also developed. Relying on the use of the Skewness coefficient and peak-peak values of the signals, corrupted time records (e.g., due to saturation, lightning, and transducer damage) are automatically discarded before modal identification.

The automated extraction was applied to eight months of vibration data coming from the installed monitoring system. Figures 7–9 show the trend of the first three eigenfrequencies of the structure. Instead, Figure 10 shows the MAC trend for the first mode. The changes of the eigenfrequencies are always lower than 5%. Furthermore, the uncertainty interval equal to $\pm 2\sigma$ (see Table 4) around the identified eigenfrequency value for the first mode is shown in Figure 11. This $\pm 2\sigma$ interval expresses a level of confidence of about 95% [45]. The width of the uncertainty intervals is clearly overestimated (indeed the cycles due to daily variability are clearly visible), which is probably due the fact that the value of σ was estimated through MCMC considering a day with very low wind (see previously in the paper). Therefore, when the wind increases (even slightly) the signal-to-noise ratio of the accelerometer signals and the accuracy of the estimations of the modal parameters improve as well. The consequence is that σ appears to be overestimated in this case.

The wind speed is proven to be able to change the eigenfrequency values significantly. Indeed, the spikes towards zero in Figures 7–9 are always related to the presence of an increased value of the root mean square (RMS) of the acceleration signals (the RMS is calculated on the frequency band of the considered mode). This RMS is strongly correlated with the wind speed (Figure 12 shows that peaks of the RMS of vibration correspond to peaks of the wind speed sensor).

It is also remarked that the eigenfrequency trends show a daily cycle due to temperature and sun exposure trends, as evidenced in Figure 13.

As for the MACs, slight decreases in time are evident. However, more data are needed (at least one year of data for a whole seasonal cycle) for a consistent analysis of such a trend. Moreover, the MAC changes are within the dispersion found with the MCMC simulations (see previously in the paper).

5. Empirical Model of the Eigenfrequencies

An empirical model to describe the behaviour of the eigenfrequencies as function of environmental factors was developed. Something similar will be performed for the mode shapes. The aim of the empirical model is to have a reliable tool

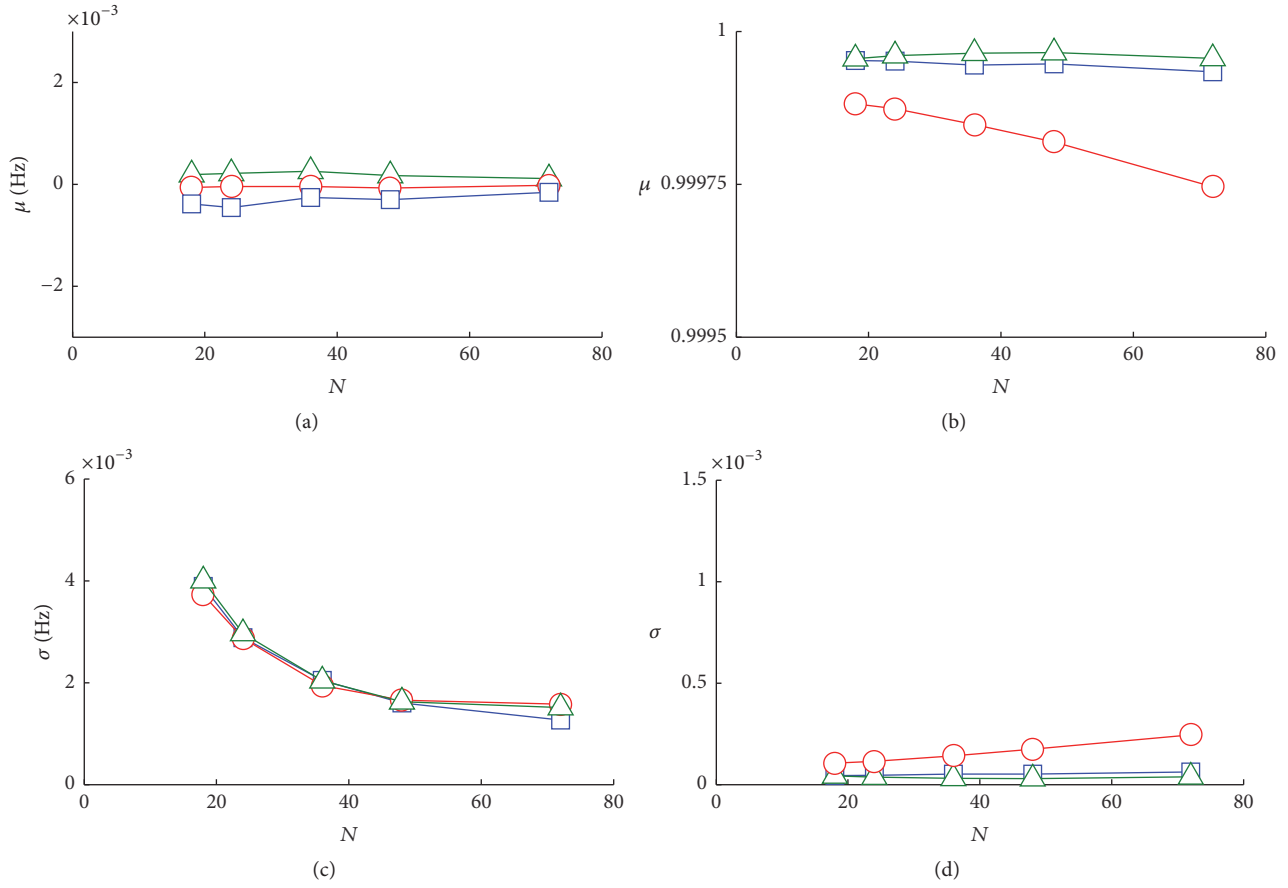

FIGURE 6: Results of the MCMC simulations for FDD as function of N ($R = 5$ mHz): mean value of the error for the eigenfrequency estimation (a), mean value of the MAC (b), σ of the error for the eigenfrequency estimation (c), and σ for the MAC (d). Curves with squares (□) for the first mode, with circles (○) for the second mode, and with triangles (△) for the third mode.

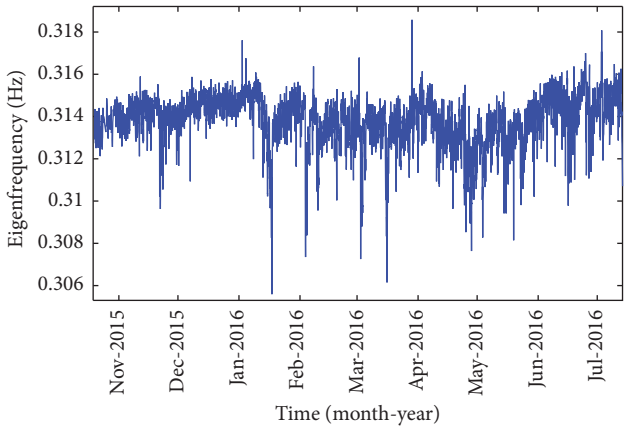

FIGURE 7: Time trend of the first eigenfrequency.

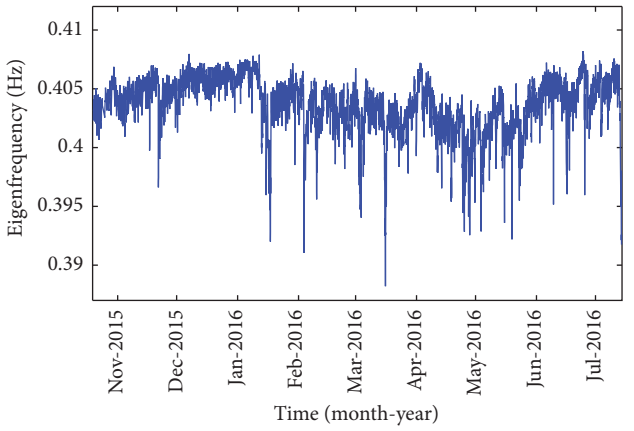

FIGURE 8: Time trend of the second eigenfrequency.

to describe the evolution of natural frequencies due to environmental factors. If the model is accurate enough, discrepancies between experimental data and model results could be employed to assess the presence of a change in the structure not due to environmental factors and thus possibly due to damage. Indeed, if a change of the eigenfrequencies could not be described by the model, a check of the building would be required.

Many correlation studies were carried out before developing the statistical model in order to understand which variables should have been used as inputs to the model: for

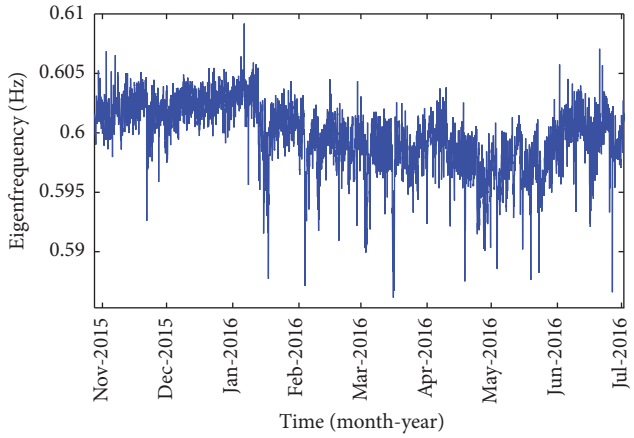

Figure 9: Time trend of the third eigenfrequency.

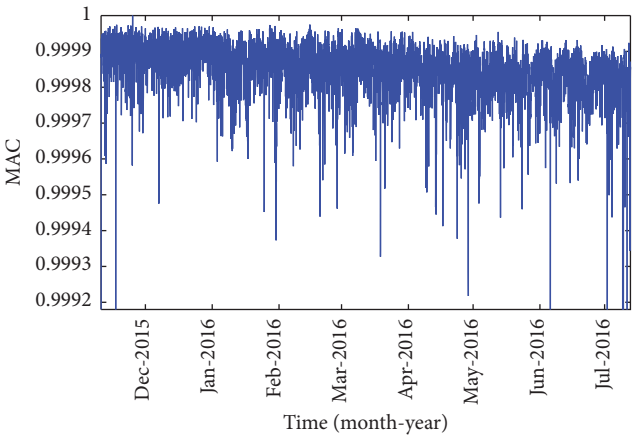

Figure 10: Time trend of the MAC of the first mode.

example, sun exposure, temperature, level of the aquifer, and wind speed and direction.

A first analysis showed that many environmental factors affect the building behaviour. Particularly, as already mentioned, the first natural frequencies can undergo shifts due to sun exposure, temperature, adjustments of the foundations, wind speed and direction, and so forth. The problem is quite complex and it is difficult to understand which parameters should be included in the empirical model for several reasons: firstly, only general information is available; for example, the authors do not have any temperature or radiation map but just a punctual value, while the acceleration sensors are distributed along the whole building. Secondly, it is important to understand which variables are correlated in order not to include them in the model and to avoid redundancy in the information. Finally, it has to be underlined that the available data do not come from a planned test but are related to the actual environmental conditions during the observation period. All these aspects make the problem difficult to approach; for this reason, the authors decided to try to reduce its complexity by considering few synthetic variables able to take into account the effect of most of the environmental parameters. To this purpose, the authors

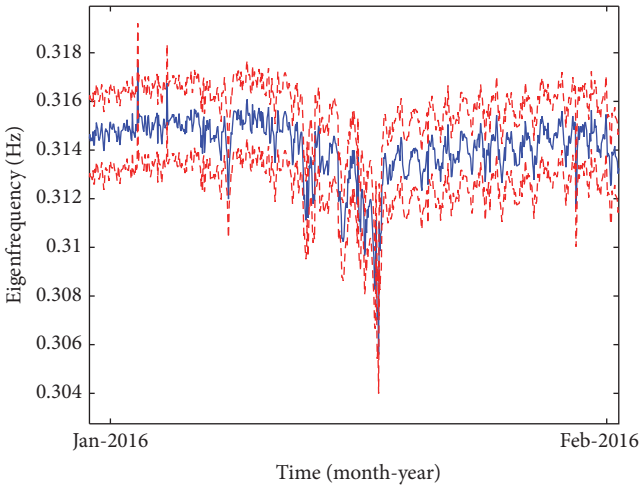

Figure 11: Trend of the first eigenfrequency (solid blue curve) and $\pm 2\sigma$ interval (dashed red curves).

selected two quantities: the acceleration RMS and the value of the building inclination. Many correlation studies were carried out, showing the correlation between these synthetic parameters and the environmental factors. Finally, the authors chose as inputs of the empirical model the following three physical quantities which demonstrated no (or negligible) correlation:

(i) The RMS A_{RMS} of the signal of the accelerometer placed in correspondence of the instrumented degree of freedom of the building with the highest mode shape component associated with the eigenfrequency considered. This allows automatically taking into account wind speed and direction. Obviously, the RMS is calculated on the frequency range of the mode considered

(ii) Inclination at the 3rd floor underground of the building I_{-3} in east-west direction (about x-axis, see Figure 1) (see Figure 14(a)). This accounts for the possible foundation adjustments

(iii) Inclination at the 30th floor of the building I_{30} in east-west direction (about x-axis, see Figure 1) (see Figure 14(b)). This accounts for sun exposure and temperature effects.

Linear regression was performed between each of the three eigenfrequencies and the three mentioned inputs. After the checks for the significance of the regression (e.g., check of the residues [47]), the model was further refined. Particularly the RMS of the accelerometer was replaced by its logarithm. Indeed, this allowed increasing significantly the correlation between the statistical model and the modal parameter values identified experimentally. Different indexes were used to quantify this correlation (e.g., PRESS [47]). Finally, the model used was

$$f_i = B_i I_{30} + C_i I_{-3} + D_i \log A_{\mathrm{RMS}}, \tag{2}$$

where f_i is the ith eigenfrequency (with $i = 1, 2, 3$), while B_i, C_i, and D_i are the constants to be determined.

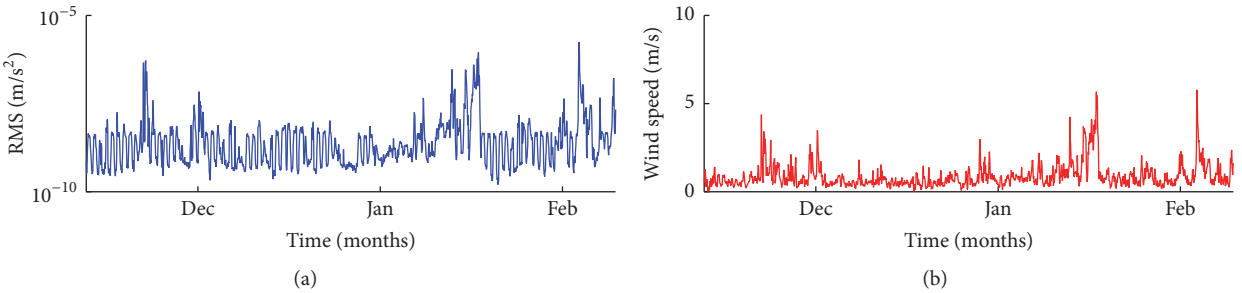

Figure 12: Trend of the vibration RMS (at floor 37 in x direction, see Figure 1) (a) and the corresponding wind speed (b).

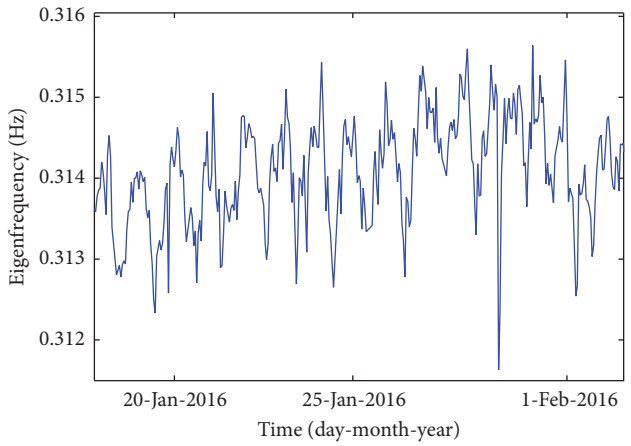

Figure 13: Trend of the first eigenfrequency where the daily changes are evident.

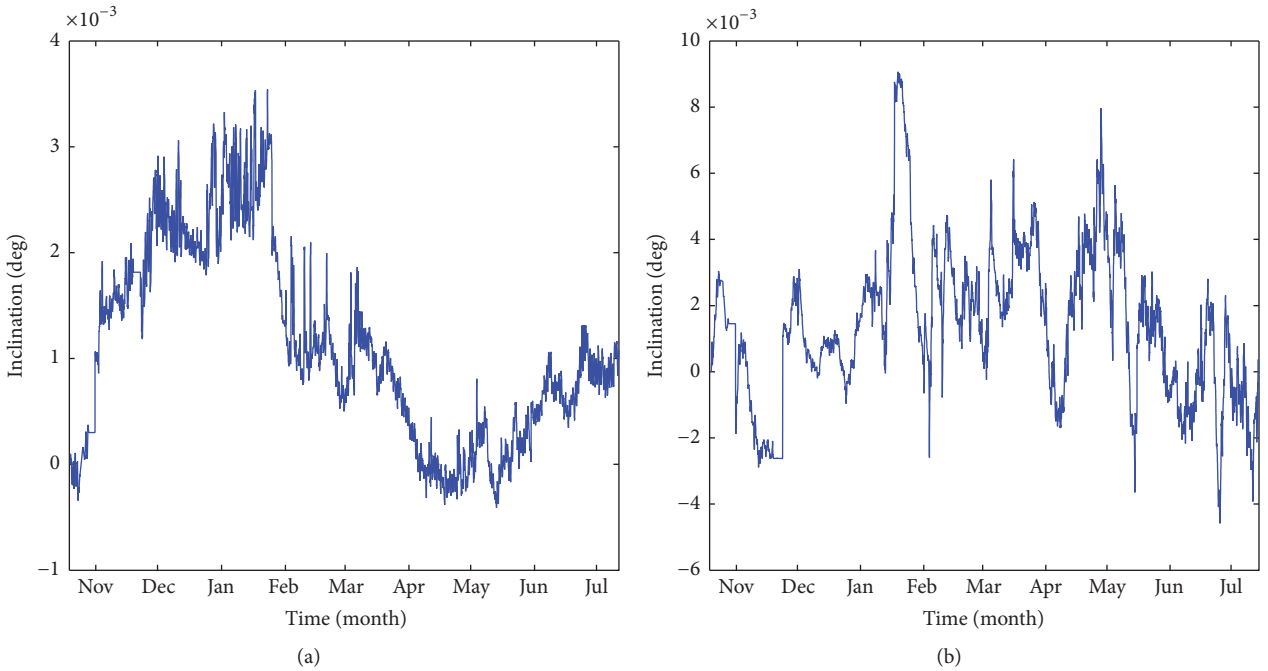

Figure 14: Trend of inclination (from a given reference value) between 2015 and 2016: inclinometer at the 3rd floor underground of the building in east-west direction (a) and at the 30th floor of the building in east-west direction (b).

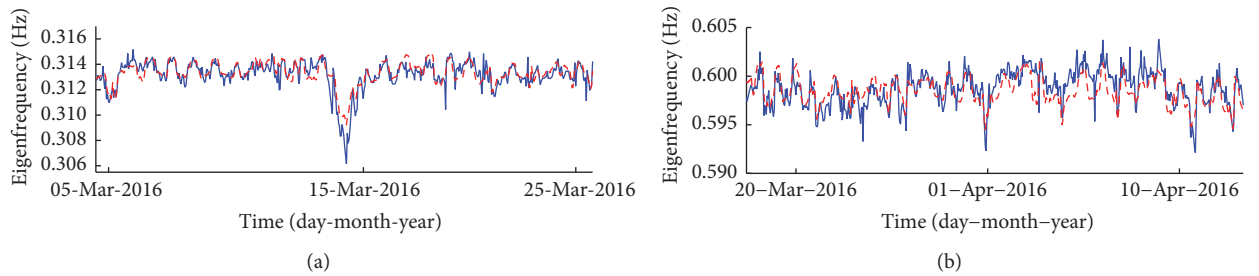

Figure 15: Trend of experimental (blue solid curves) and reconstructed (red dashed curves) eigenfrequencies: first eigenfrequency (a) and third eigenfrequency (b).

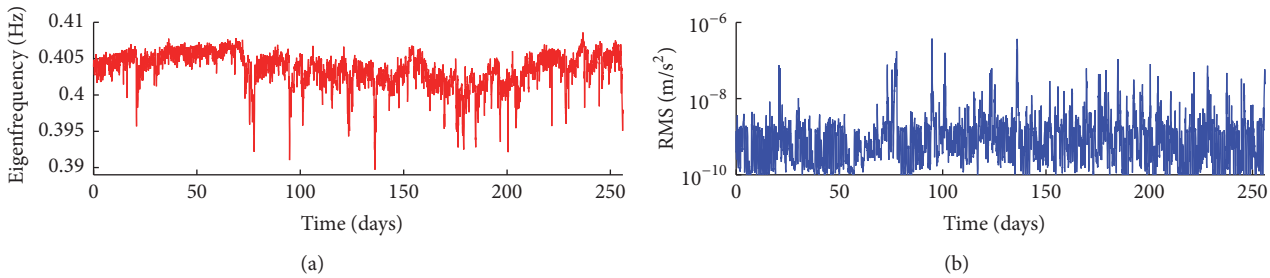

Figure 16: Experimental trend of the second eigenfrequency (a) and the vibration RMS at floor 37 in x direction (see Figure 1) calculated on the frequency range of the second eigenfrequency (b).

However, the correlation level must be further increased (and confidence intervals must be estimated [47]). To do this, more data are needed to find out all the possible input parameters that must be considered in the model as well as possible transformations (e.g., application of logarithm).

Nevertheless, the current version of the model shows a moderately satisfactory behaviour (see Figure 15). The sudden changes of the eigenfrequency value are shown to be mainly due to the acceleration RMS value (as already mentioned and as also evidenced by Figure 16, where the peaks of the vibration RMS correspond to sudden decreases of the eigenfrequency considered), while the values of inclination are able to properly describe the long-time trends (from daily trends to seasonal trends), as expected.

When more data coming from the system will be available, they will be used to further improve the model presented herein.

6. Conclusion

The paper has described the monitoring system installed and a proposed data analysis strategy for Palazzo Lombardia, one of the tallest buildings in Milano. The layout of the system is presented, highlighting the measured variables and therefore the data available for a health monitoring strategy.

An approach based on automatic and continuous modal parameter extraction has then been presented. The main features of the automatic modal analysis software used for modal identification are then provided, explaining how Markov Chain Monte Carlo simulations were used to optimise it.

This automatic identification system allowed producing the first plots of the trends of the modal parameters of the building along eight months of monitoring. These modal parameters allowed the authors to develop a first-attempt empirical model to describe the relationship between the first three eigenfrequencies of the building and a number of input variables representative of the environmental conditions. The statistical model proved to be able to estimate the predicted values for the identified frequencies as a function of environmental conditions and therefore could be used (after its improvement) to detect anomalous trends indicating a change in the structure.

Conflicts of Interest

The authors declare that there are no conflicts of interest regarding the publication of this paper.

Acknowledgments

The authors wish to acknowledge the Lombardia Government authority and the people at CarboThermo group (facility manager) for the support given.

References

[1] E. Mesquita, P. Antunes, F. Coelho, P. André, A. Arêde, and H. Varum, "Global overview on advances in structural health monitoring platforms," *Journal of Civil Structural Health Monitoring*, vol. 6, no. 3, pp. 461–475, 2016.

[2] D. Duarte, B. Marado, J. Nogueira, B. Serrano, V. Infante, and F. Moleiro, "An overview on how failure analysis contributes to flight safety in the Portuguese Air Force," *Engineering Failure Analysis*, vol. 65, pp. 86–101, 2016.

[3] C. R. Farrar and K. Worden, *Structural Health Monitoring: A Machine Learning Perspective*, Wiley, 2012.

[4] S. Da Silva, M. Todd, J. S. Sakellariou, and M. Ghandchi-Tehrani, "The use of vibration signals for structural health monitoring, system identification, test planning/optimization, and dynamic model validation/updating," *Shock and Vibration*, vol. 2016, Article ID 9581650, 2 pages, 2016.

[5] O. S. Salawu, "Detection of structural damage through changes in frequency: a review," *Engineering Structures*, vol. 19, no. 9, pp. 718–723, 1997.

[6] D. P. Patil and S. K. Maiti, "Detection of multiple cracks using frequency measurements," *Engineering Fracture Mechanics*, vol. 70, no. 12, pp. 1553–1572, 2003.

[7] Z. Yang and Le Wang, "Structural damage detection by changes in natural frequencies," *Journal of Intelligent Material Systems and Structures*, vol. 21, no. 3, pp. 309–319, 2010.

[8] A. K. Pandey, M. Biswas, and M. M. Samman, "Damage detection from changes in curvature mode shapes," *Journal of Sound and Vibration*, vol. 145, no. 2, pp. 321–332, 1991.

[9] C. P. Ratcliffe, "A frequency and curvature based experimental method for locating damage in structures," *Journal of Vibration and Acoustics*, vol. 122, no. 3, pp. 324–329, 2000.

[10] C. S. Hamey, W. Lestari, P. Qiao, and G. Song, "Experimental damage identification of carbon/epoxy composite beams using curvature mode shapes," *Structural Health and Monitoring*, vol. 3, no. 4, pp. 333–353, 2004.

[11] M.-K. Yoon, D. Heider, J. W. Gillespie Jr., C. P. Ratcliffe, and R. M. Crane, "Local damage detection with the global fitting method using mode shape data in notched beams," *Journal of Nondestructive Evaluation*, vol. 28, no. 2, pp. 63–74, 2009.

[12] G. Li, K. Hao, Y. Lu, and S. Chen, "A flexibility approach for damage identification of cantilever-type structures with bending and shear deformation," *Computers & Structures*, vol. 73, no. 6, pp. 565–572, 1999.

[13] Z. G. Zhou, L. D. Wegner, and B. F. Sparling, "Vibration-based detection of small-scale damage on a bridge deck," *Journal of Structural Engineering—ASCE*, vol. 133, no. 9, pp. 1257–1267, 2007.

[14] J. Li, B. Wu, Q. C. Zeng, and C. W. Lim, "A generalized flexibility matrix based approach for structural damage detection," *Journal of Sound and Vibration*, vol. 329, no. 22, pp. 4583–4587, 2010.

[15] Z. Y. Shi, S. S. Law, and L. M. Zhang, "Structural damage localization from modal strain energy change," *Journal of Sound and Vibration*, vol. 218, no. 5, pp. 825–844, 1998.

[16] N. Stubbs and J.-T. Kim, "Improved damage identification method based on modal information," *Journal of Sound and Vibration*, vol. 252, no. 2, pp. 223–238, 2002.

[17] S. Choi, S. Park, N.-H. Park, and N. Stubbs, "Improved fault quantification for a plate structure," *Journal of Sound and Vibration*, vol. 297, no. 3-5, pp. 865–879, 2006.

[18] G. Tondreau and A. Deraemaeker, "Numerical and experimental analysis of uncertainty on modal parameters estimated with the stochastic subspace method," *Journal of Sound and Vibration*, vol. 333, no. 18, pp. 4376–4401, 2014.

[19] M. Ralbovsky, M. Kwapisz, and A. Vorwagner, "Uncertainty of bridge vibration properties and its consequence for damage identification," in *Proceedings of the 5th ECCOMAS Thematic Conference on Computational Methods in Structural Dynamics and Earthquake Engineering, COMPDYN 2015*, pp. 2545–2557, May 2015.

[20] J. Kullaa, "Structural health monitoring under nonlinear environmental or operational influences," *Shock and Vibration*, vol. 2014, Article ID 863494, 9 pages, 2014.

[21] G. Comanducci, F. Ubertini, and A. L. Materazzi, "Structural health monitoring of suspension bridges with features affected by changing wind speed," *Journal of Wind Engineering & Industrial Aerodynamics*, vol. 141, pp. 12–26, 2015.

[22] N. Dervilis, H. Shi, K. Worden, and E. J. Cross, "Exploring environmental and operational variations in SHM data using heteroscedastic Gaussian processes," in *Proceedings of the 34th IMAC, Conference and Exposition on Structural Dynamics, 2016*, vol. 2, pp. 145–152, January 2016.

[23] C. Devriendt, F. Presezniak, G. De Sitter et al., "Structural health monitoring in changing operational conditions using tranmissibility measurements," *Shock and Vibration*, vol. 17, no. 4-5, pp. 651–675, 2010.

[24] X. Zhu and H. Hao, "Development of an integrated structural health monitoring system for bridge structures in operational conditions," *Frontiers of Structural and Civil Engineering*, vol. 6, no. 3, pp. 321–333, 2012.

[25] C. Rainieri and G. Fabbrocino, *Operational Modal Analysis of Civil Engineering Structures*, Springer, New York, NY, USA, 2014.

[26] B. Peeters, H. Van Der Auweraer, P. Guillaume, and J. Leuridan, "The PolyMAX frequency-domain method: a new standard for modal parameter estimation?" *Shock and Vibration*, vol. 11, no. 3-4, pp. 395–409, 2004.

[27] R. Brincker, L. Zhang, and P. Andersen, "Modal identification of output-only systems using frequency domain decomposition," *Smart Materials and Structures*, vol. 10, no. 3, pp. 441–445, 2001.

[28] M. Berardengo, A. Cigada, S. Manzoni, and M. Vanali, "design and installation of a permanent monitoring system for Palazzo Lombardia in Milano, Italy," in *Proceedings of the VII European Congress on Computational Methods in Applied Sciences and Engineering - ECCOMAS Congress 2016*, pp. 3640–3651, Crete Island, Greece, June 2016.

[29] A. Cigada, E. Mola, F. Mola, G. Stella, and M. Vanali, "Dynamic behavior of the palazzo lombardia tower: Comparison of numerical models and experimental results," *Journal of Performance of Constructed Facilities*, vol. 28, no. 3, pp. 491–501, 2014.

[30] ISO2631-1, *Mechanical vibration and shock - Evaluation of Human Exposure to Whole-Body Vibration - Part 1: General Requirements*, 1997.

[31] L. G. Griffis, "Serviceability limit states under wind load," *Engineering Journal*, vol. 30, no. 1, pp. 1–16, 1993.

[32] P. Mendis, T. Ngo, N. Haritos, A. Hira, B. Samali, and J. Cheung, "Wind loading on tall buildings," *Electronic Journal of Structural Engineering Special Issue: Loading on Structures*, vol. 3, pp. 41–54, 2007.

[33] G. Busca, A. Cigada, E. Mola, F. Mola, and M. Vanali, "Dynamic testing of a helicopter landing pad: Comparison between operational and experimental approach," *Journal of Civil Structural Health Monitoring*, vol. 4, no. 2, pp. 133–147, 2014.

[34] S. Campagnari, F. di Matteo, S. Manzoni, M. Scaccabarozzi, and M. Vanali, "Estimation of axial load in tie-rods using experimental and operational modal analysis," *Journal of Vibration and Acoustics*, vol. 139, no. 4, article 041005, 2017.

[35] G. James III, T. Carne, and J. Lauffer, "The natural excitation technique (next) for modal parameter extraction from operating structures," *The International Journal of Analytical and Experimental Modal Analysis*, vol. 10, no. 4, pp. 260–277, 1995.

[36] F. Ubertini, C. Gentile, and A. L. Materazzi, "Automated modal identification in operational conditions and its application to bridges," *Engineering Structures*, vol. 46, pp. 264–278, 2013.

[37] T. Wang, O. Celik, F. N. Catbas, and L. M. Zhang, "A frequency and spatial domain decomposition method for operational strain modal analysis and its application," *Engineering Structures*, vol. 114, pp. 104–112, 2016.

[38] C. Devriendt and P. Guillaume, "Identification of modal parameters from transmissibility measurements," *Journal of Sound and Vibration*, vol. 314, no. 1-2, pp. 343–356, 2008.

[39] A. Brandt, M. Berardengo, S. Manzoni, and A. Cigada, "Harmonic scaling of mode shapes for operational modal analysis," in *Proceedings of the ISMA 2016 - International Conference on Noise and Vibration Engineering and USD2016 - International Conference on Uncertainty in Structural Dynamics*, pp. 2809–2818, Leuven, Belgium, September 2016.

[40] C. Rainieri and G. Fabbrocino, "Development and validation of an automated operational modal analysis algorithm for vibration-based monitoring and tensile load estimation," *Mechanical Systems and Signal Processing*, vol. 60, pp. 512–534, 2015.

[41] D. J. Ewins, *Modal testing: Theory, Practice and Application*, Baldock: Research Studies Press Ltd., 2nd edition, 2000.

[42] J. S. Bendat and A. G. Piersol, *Engineering Applications of Correlation and Spectral Analysis*, Wiley-Interscience, New York, NY, USA, 1993.

[43] A. Brandt, *Noise and Vibration Analysis—Signal Analysis and Experimental Procedures*, John Wiley & Sons, Chichester, UK, 2011.

[44] G. D'Antona and A. Ferrero, *Digital Signal Processing for Measurement Systems: theory and Applications (Information Technology: Transmission, Processing and Storage)*, Springer, New York, NY, USA, 2006.

[45] JCGM 100:2008, *Evaluation of Measurement Data—Guide to the Expression of Uncertainty in Measurement*, 2008.

[46] JCGM101:2008, *Evaluation of Measurement Data—Supplement 1 to the Guide to the Expression of Uncertainty in Measurement—Propagation of Distributions Using a Monte Carlo Method*, 2008.

[47] D. C. Montgomery, *Design and Analysis of Experiments*, John Wiley & Sons, 7th edition, 2009.